Nep J Environ Sci (2025), 13(1), 43-60
https://doi.org/10.3126/njes.v13i1.69072
ISSN 2350-8647 (Print) 2542-2901 (Online)

Research Article

Application of the Bivariate Frequency Ratio Method for Landslide Susceptibility Mapping of Manthali Municipality, Ramechhap District, Nepal

Tara Ale Magar[1], Bharat Prasad Bhandari[1,2]
[1]College of Applied Sciences, Tribhuvan University, Kathmandu, Nepal
[2]Central Department of Environmental Science, Institute of Science and Technology, Tribhuvan University, Kathmandu, Nepal

(Received: 23 August 2024; Revised: 25 June 2025; Accepted: 28 June 2025)

Abstract
This study intends to create a landslide susceptibility map for Manthali Municipality in Ramechhap District, Nepal, utilizing the frequency ratio method. The landslide inventory map was developed using Google Earth and Landsat satellite imagery, with a 70% allocation for training data and 30% for testing data. The inventory map has been finalized subsequent to the field verification process. The assessment of landslide distribution encompassed the evaluation of ten variables, including slope, aspect, elevation, geology, proximity to roads and streams, curvature, land cover, topographical wetness index and precipitation patterns. The definitive weight for each factor was obtained from the raster analysis tool in ArcGIS. The resultant map was classified into four distinct susceptibility categories: low, moderate, high, and very high. The result was validated using the area under the curve method. The results demonstrate that the classifications of low, moderate, high, and very high accounted for 40.8%, 38.64%, 17.64%, and 2.92% of the total area, respectively. The area under the receiver operating characteristic curve (AUC) for the success rate was calculated at 78.94%, whereas the prediction rate was evaluated at 74.06%. The results indicate a significant level of predictive accuracy. The designated study area can utilize the generated landslide susceptibility map for effective landslide mitigation, strategic land use planning, and efficient settlement management.

Keywords: *DEM, frequency ratio, landslide susceptibility, Manthali*

Introduction
Landslides are a natural calamity that causes considerable fatalities and property loss in numerous regions globally (Li et al., 2022). Although it is unattainable to entirely avert natural disasters such as earthquakes, floods, and landslides, it is possible to mitigate the severity of the processes and their resultant effects. The predominant geological event is a landslide, occurring globally and characterized by the displacement of land. They may occur when substantial quantities of dirt, rocks, or debris descend a slope due to natural phenomena or human activities (Cruden, 1991). Landslides, mostly identified as rock falls, rockslides, debris flows, and mudslides, are recognized as one of the most substantial hazards in Nepal. This is especially accurate in the hilly areas of Nepal situated on steep slopes and concave surfaces (Bhandari et al., 2024; Ayer & Bhandari, 2024). According to disaster portal of Ministry of Home Affairs in Nepal, 92 individuals perished, 80 sustained injuries, and 1,968 residential properties were affected by landslides in the year 2021. These occurrences culminated in a significant economic loss of USD 1,311,267 in Nepal. Landslide occurrence is a highly complex process influenced by various factors, including geological conditions, lithological associations, topographical features, hydrological conditions, seismic activity, and anthropogenic interventions (Bhandari & Dhakal, 2018, Bhandari & Dhakal, 2019; Bhandari & Dhakal, 2021).

The creation of landslide susceptibility maps by the use of suitable models and the selection of effective conditioning variables is a widely employed strategy for mitigating landslide-related damage (Dam et al., 2022). A multitude of studies including both qualitative and quantitative methodologies have advanced the creation of landslide susceptibility maps in recent decades. The frequency ratio model is a widely utilized model with a superior success rate and enhanced predictive accuracy among bivariate models (Pal & Chowdhuri, 2019; Thapa & Bhandari, 2019; Acharya et al., 2017; Silalahi et al., 2019; Addis, 2023; Ayer & Bhandari, 2024; Bhandari et al., 2024). In landslide susceptibility mapping, multiple bivariate models can be evaluated to select the superior model based on higher success and prediction rates. The bivariate frequency ratio and weight of evidence models, along with the frequency ratio and information value models, constitute the basis for the construction of landslide susceptibility models (Addis, 2023; Bhandari et al., 2024). The calculation and visualization of the cumulative impacts of conditioning variables on landslides can be enhanced through the utilization of GIS software. This study used a frequency ratio (FR) model to generate landslide susceptibility maps for the Manthali Municipality in Ramechhap District, Nepal. The results of this study can aid decision-makers in pinpointing areas within the study region that are

*Corresponding author: bbhandari@cdes.edu.np

susceptible to landslides, which is essential for effectively addressing these issues.

Materials and Methods

Study Area

Manthali Municipality, situated within the Ramechhap District, encompasses an area of approximately 212.74 square kilometers. It is geographically defined by its coordinates, extending from 27°18' 56.32" N to 27°30' 7.97" N latitude and from 86°1'19.47" E to 86°1'41.65" E longitude. This municipality is bordered to the east by Ramechhap Municipality, to the west by Khadadevi and Doromba Rural Municipality, to the north by Likhu Tamakoshi Rural Municipality, and to the south by Melung Village Municipality in Dolakha District and Golanjar Rural Municipality in Sindhuli District (Fig. 1).

The region under examination exhibits a climate that ranges from subtropical to alpine. The typical temperature within the study area fluctuates between 20 °C and 25 °C, accompanied by an annual average precipitation of 1315 mm. The rainfall stations in proximity to the study area include Manthali, Melung, and Sindhulimadi, identified by the index numbers 112301, 1104, and 1107, respectively. The Sunkoshi River, Tamakoshi River, Bhatauli, and Ranjor River constitute the principal waterways within the scope of this study area.

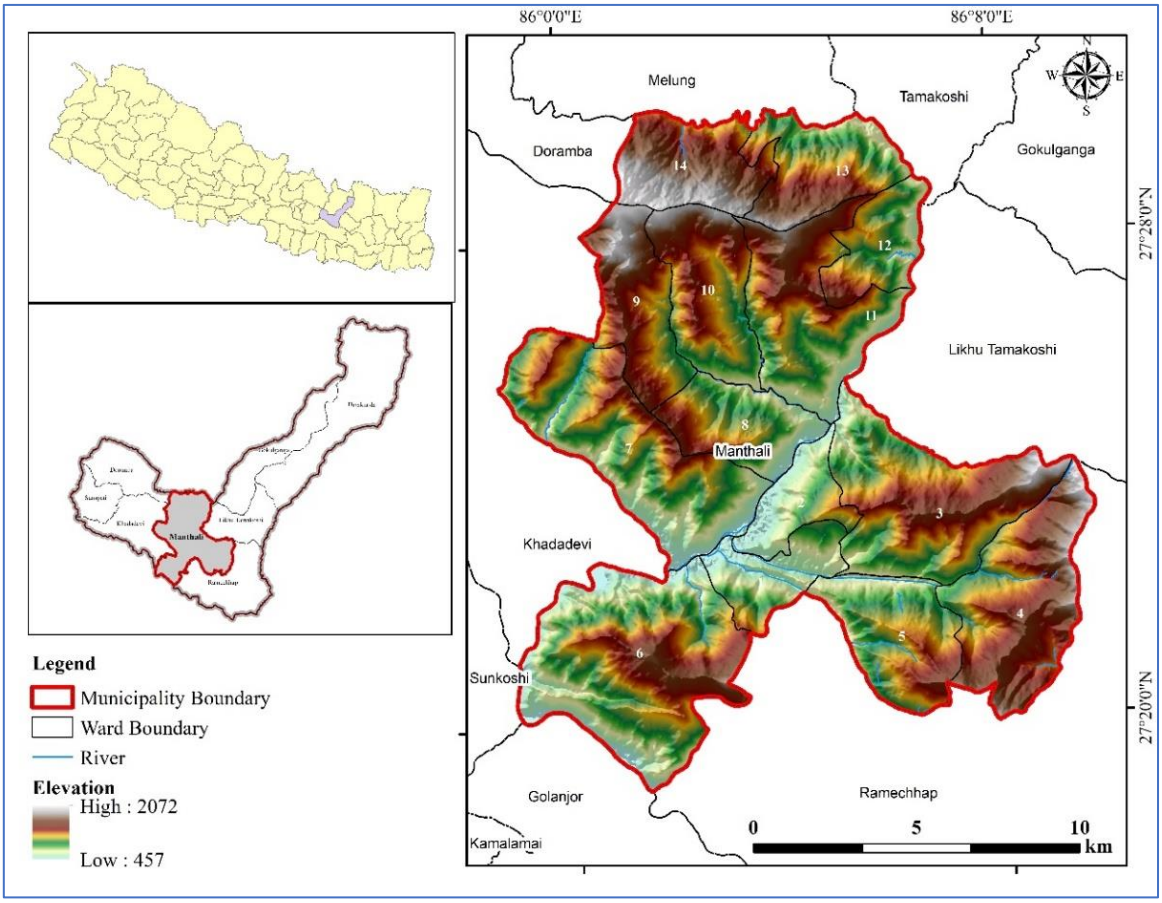

Figure 1. Location Map of Manthali Municipality

Methods

Primary data

The primary data was gathered by field observations employing equipment like GPS devices and a structured checklist. The preliminary field visit concentrated on surface mapping of the research region, aiding in the creation of the landslide inventory map. The field visit was performed to finalize the landslide susceptibility map and identification of historical landslides in the study region. More than 70% of identified landslides were confirmed in the field via eye inspection and community discussions.

Secondary data

An extensive collection of secondary data sources was analyzed to gather pertinent information. The research analyzed the topographical characteristics and relevant data of the study region using topo-sheet number 2786 09C (RAMECHHAP) at a scale of 1:25,000. The geological map was acquired from the Department of Mines and Geology (DMG), Government of Nepal. This study's analysis utilized historical time-based imagery acquired from Google Earth. A 30-meter digital elevation model (DEM) from the United States Geological Survey (USGS) was utilized to generate the factor maps. The meteorological data was acquired from

the Department of Hydrology and Meteorology (DHM) at the Sindhulimadi, Melung, and Manthali locations. Data from a single station cannot produce an accurate rainfall map; therefore, rainfall stations in the neighborhood of the study area were utilized for collecting the rainfall data.

The dataset consists of monthly precipitation observations gathered over 30 years, specifically from 1990 to 2020, from three neighboring meteorological stations. The Inverse Distance Weighted (IDW) interpolation method was utilized to analyze rainfall data within a Geographic Information System (GIS) to estimate precipitation values across the specified research area.

Remote sensing data

Slope and aspect were determined for the study region using the Advanced Space Borne Thermal Emission and Reflection Radiometer (ASTER) Digital Elevation Model (DEM) obtained from USGS with spatial resolution of 30 meters. Google Earth Pro and Landsat-8 created an inventory of landslides and a map of the land's surface.

Landslide inventory

The landslide inventory map for the study area was created by digitizing landslide features observed in satellite imagery obtained from Google Earth. First of all, the old and new scar of the landslides was identified from the imagery. The conformed scars were traced out into imageries based on the polygon. The conformed old scars were verified in the field with direct visualization and public interaction. Landslides were systematically categorized into training (70%) and testing (30%) datasets, with each landslide meticulously delineated as a polygon and subsequently imported into ArcGIS for comprehensive analysis. The polygons were transformed into raster format and projected utilizing the WGS 1984 UTM Zone 44N coordinate system to ensure spatial consistency. The mapping was carried out at a scale of 1:25,000, providing an effective balance between spatial detail and interpretability for hazard analysis at the municipal level in mountainous areas. Field surveys were conducted to corroborate and authenticate the mapped landslides. The training dataset comprised 70% of historical landslides that occurred before 2018, whereas the testing dataset accounted for 30% of recent active landslides occurred after 2018. The reclassification of each causative factor map was conducted, and the pixel area for each class was documented. The landslide pixel area was subsequently calculated by cross-tabulating these with the landslide inventory. The resulting values were utilized to implement the Frequency Ratio (FR) model for susceptibility analysis.

Landslide causative factors

The local topography, geology, tectonic characteristics, weather conditions, land use, and human activities are crucial in ascertaining the geographical distribution and severity of landslides. Therefore, it is essential to assess the influence of these causal factors on the spatial distribution of landslides to understand their mechanisms and, ultimately, to develop a landslide susceptibility map. Numerous researchers employed over 10 causative factors, including geological, land cover, topographical, and hydrological elements, to create the landslide susceptibility map for the Nepal Himalaya (Bhandari et al., 2024). According to the literature and preliminary field survey, ten causative elements were identified to create the landslide susceptibility map.

Topographical wetness index

The distribution of soil moisture is influenced by topographic characteristics, and the flow of groundwater is generally regulated by surface topography (Burt & Butcher, 1986; Seibert et al., 1997; Zinko et al., 2005). As a result, scholars have employed topographic markers to clarify the geographical distribution of soil moisture (Burt & Butcher, 1986; Moore et al., 1991). Beven and Kirkby (1979) first developed the Topographic Wetness Index (TWI) as a component of the TOP MODEL runoff model. This measure, known as the Topographic Wetness Index (TWI), is commonly used to evaluate the impact of topography on hydrological processes. This control is measured by integrating the local upslope contributing area with the overall slope. The topographical wetness index (TWI) as the natural logarithm of the ratio between the parameter "a" and the tangent of the angle "β".

$$TWI = \ln (a / \tan \beta) \qquad \text{Eq. (1)}$$

The variable "a" represents the cumulative upslope area that is drained through a certain point, measured per unit contour length. The variable "tan β" represents the slope angle at the same point. This phenomenon influences the spatial distribution of soil moisture, and groundwater movement frequently aligns with surface topography. In the present study, the role of TWI was examined as an additional influential element (Fig. 2).

Slope

According to Shafique et al. (2016), the slope of the terrain has a significant role in determining the geographical distribution and intensity of landslides. ASTER data and GIS were utilized to ascertain the incline of the research area's terrain. The determination was made with the algorithm proposed by Burroughs and McDonnell (1998). The gradient map is partitioned into five distinct subcategories ranging from 0 to 67 degrees (Fig. 3). Slope has played significant role to cause landslide in the Himalaya where the landslide susceptibility increases with increasing hillslope (Bhandari & Dhakal, 2020, Ayer & Bhandari 2024, Dhakal & Tamang 2024). Increasing the hills lope causes the increment of shear force and decrease in the angle of internal friction so that the condition of slope instability increases (Bhandari & Dhakal, 2019).

Curvature

According to Lee and Min (2001), Lee et al. (2004), the curvature values serve as indicators of topographic morphology. The curvature map, as seen in Figure 4, was obtained by the utilization of Geographic Information System (GIS) methods, utilizing a Digital Elevation Model (DEM). The presented map categorizes the topography into three unique classifications: concave, convex, and flat regions. It is important to acknowledge that areas characterized by a convex or concave slope have a tendency to amass a greater amount of water and retain it for a prolonged period, as emphasized by Lee and Talib (2005). A positive or negative connection can be observed between the magnitude of values and the probability of a landslide event, where larger values indicate a higher risk of occurrence.

On the other hand, regions characterized by flat terrain exhibit a notably decreased probability of experiencing landslides. A positive curvature indicates the presence of an upward convexity on the surface at the specified grid point. It is important to highlight that a flat surface is denoted by a value of zero, whereas a concave surface at the top of the grid signifies a negative curvature.

Distance to Road

Destabilization of slopes and consequent landslides are common outcomes of communication network construction in mountainous regions (Shafique et al., 2016). The road network was obtained from a publicly available street map and then verified on-site in order to evaluate its effect on landslides in the specified study area. Figure 5 shows the result of using ArcGIS software to compute the distance from the road at intervals of 100 m. According to the actual conditions on the ground, a 100 m interval is used for the distance to road study. Regular vibration and stress from heavily loaded vehicles can create landslides, making areas up to 100 meters from the road appear extremely vulnerable. New landslides and the reactivation of older ones are both increased in the Himalayan region due to factors such as the close proximity to roads near by 100 m (Pokharel & Bhandari, 2019).

Distance to Drainage

The presence of streams can have detrimental effects on the stability of a slope, as they can lead to erosion-induced undercutting and increased water penetration, resulting in saturation of the slope's toe (Germer et al., 2011). The study area's stream network was calculated using ASTER DEM's Arc Hydro tool (ESRI, 2017) to assess the impact of streams on the distribution of landslides. Extraction was performed on streams that have an accumulated area above 20 km^2. The ArcGIS program was used to split the distance from the streams into six buffer zones, each separated by a 20-meter spacing (Fig. 6). The causative variables for these landslides were compared to the existing inventory of landslides in order to assess their influence on the spatial distribution of landslides and generate a map illustrating the vulnerability to landslides.

Elevation

Elevation is a significant topographic variable that plays a crucial role in determining slope stability and the likelihood of landslides. Additionally, it plays a crucial part in the features of precipitation (Corominas et al., 2014; Pourghasemi & Rahmati, 2018). The relationship between the occurrence of landslides and height is inversely proportional. The susceptibility to landslides is influenced by elevation variables, since greater elevations increase the likelihood of a landslide occurring. The components were extracted from the Digital Elevation Model (DEM) and classified into five distinct categories, as seen in Figure 7.

Rainfall

Rainfall is one of the parameters that cause decreased slope stability as it increases soil moisture conditions. Rainfall data describes the amount of water that falls to the ground surface during a certain period and is measured in units of millimeters (mm) (Fell et al., 2008). Rainfall data from the Department of Hydrology and Meteorology of 30 years from 1990 to 2020 of three stations were used to classify rainfall amounts in the study area. The higher the frequency of rainfall, the higher the chances of landslides, as shown in Figure 8. Rainfall is the major cause to occur landslide in the Nepal Himalaya during monsoon season due to abrupt loss of cohesion and angle of internal friction of the soil and rock (Dahal et al., 2008; Bhnadari & Dhakal, 2021)

Aspect

The terrain aspect is the slope direction and can influence landslide initiation due to its effect on vegetation cover, moisture retention, and soil strength (Garcia-Rodriguez et al., 2008; Silalahi, 2019). Similarly, the terrain aspect was also obtained from DEM of 30m resolution. (Fig. 9).

Geology

The likelihood of landslides is associated with the physical characteristics of both surface and subsurface materials, such as their strength and permeability, as evidenced by comprehensive study (Yang, 2018). The landslide occurrences in the Himalayas are primarily influenced by stratigraphy and geology, as these factors, along with slope and moisture levels, are interrelated (Bhandari & Dhakal, 2018). The geological map was acquired from the Department of Mines and Geology and digitized into the GIS layer. The region is geologically categorized into six formations as mentioned in figure 10.

Land Use/ Land Cover Map

Land cover substantially influences landslide distribution; generally, forest regions exhibit fewer landslides compared to non-forest areas. Vegetated land cover with a strong root system provides mechanical and hydrological benefits that often stabilize slopes (Garca-Rodrguez et al., 2008). The land cover of the analyzed region was digitized from the obtained Landsat-8 image and subsequently field-verified (Fig. 11). The land cover of the region is classified as water body, woodland, shrub

land, grassland, built-up areas, barren land, and agricultural ground.

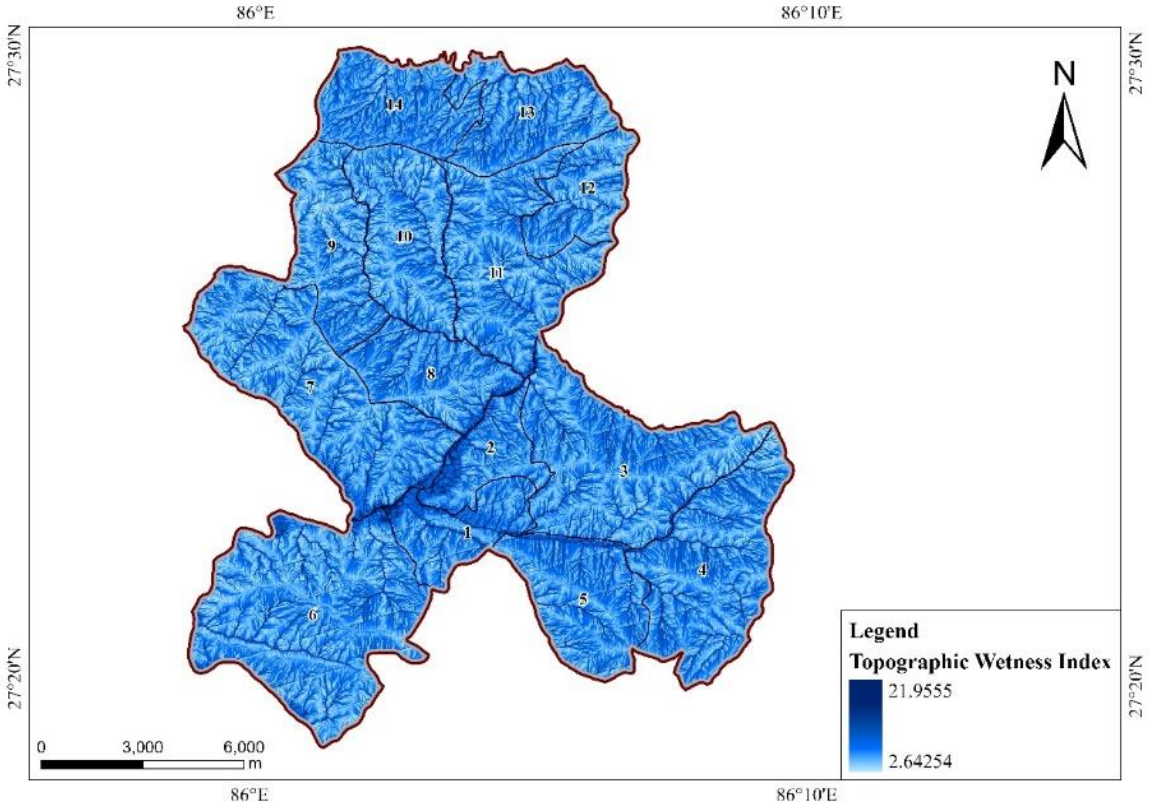

Figure 2. Topographic Wetness Index Map

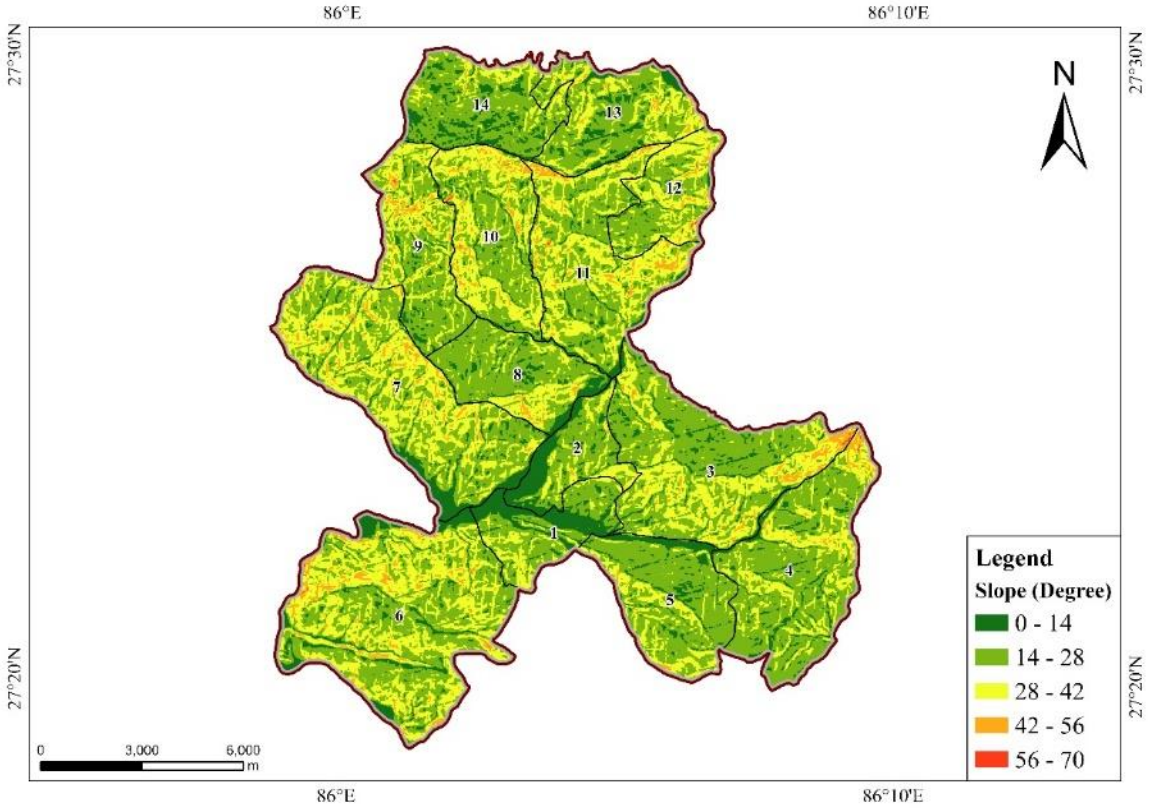

Figure 3. Slope angle map

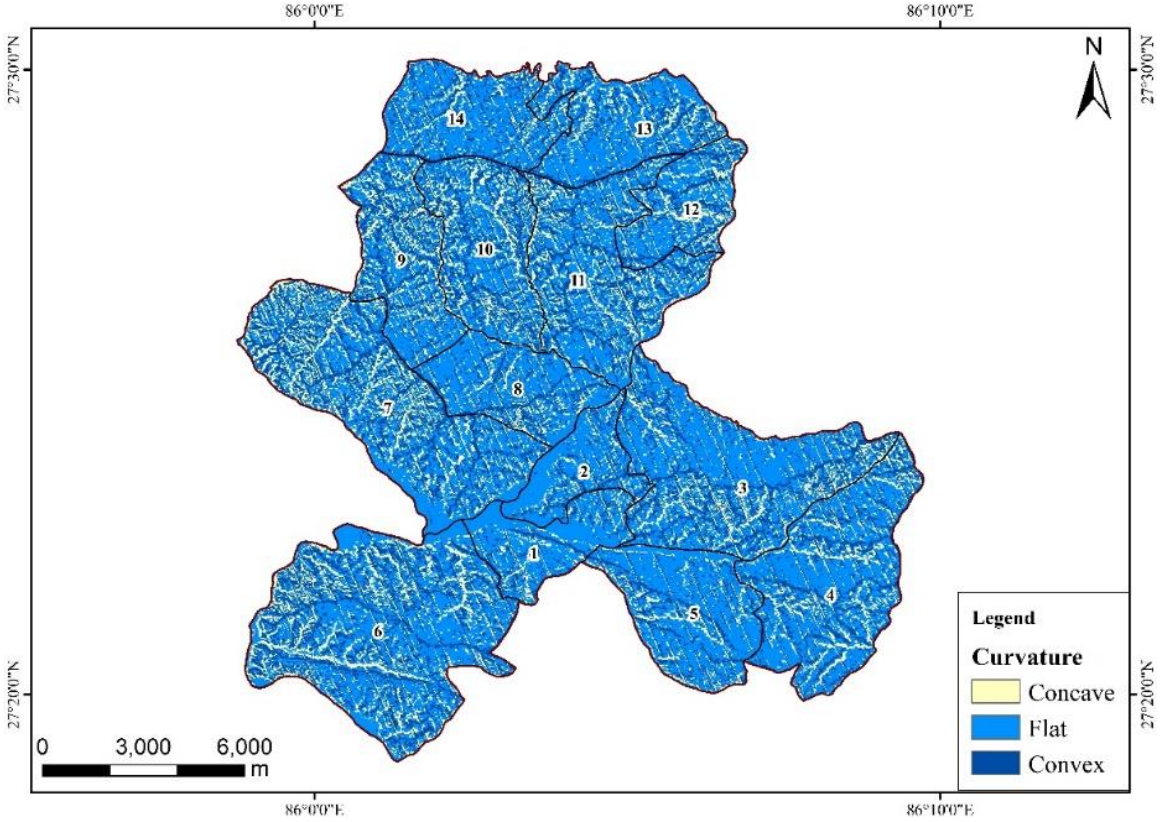

Figure 4. Curvature map

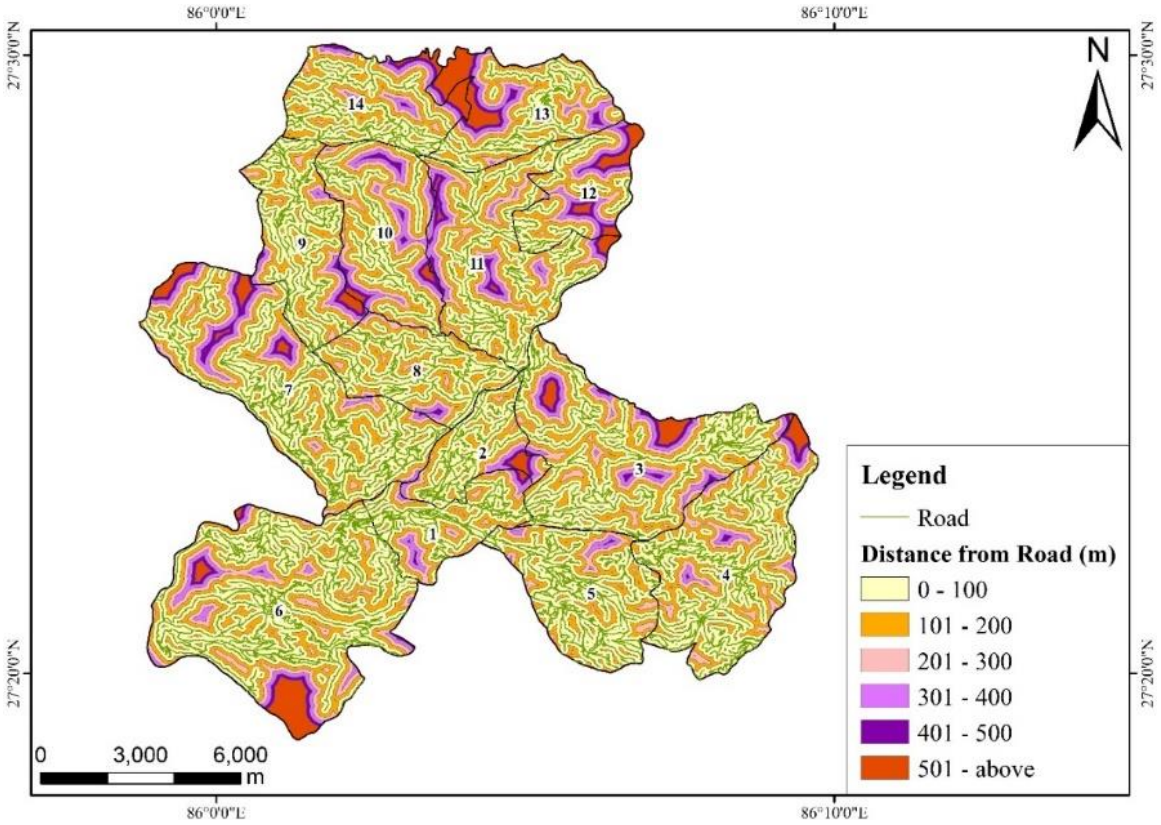

Figure 5. Distance from Road map

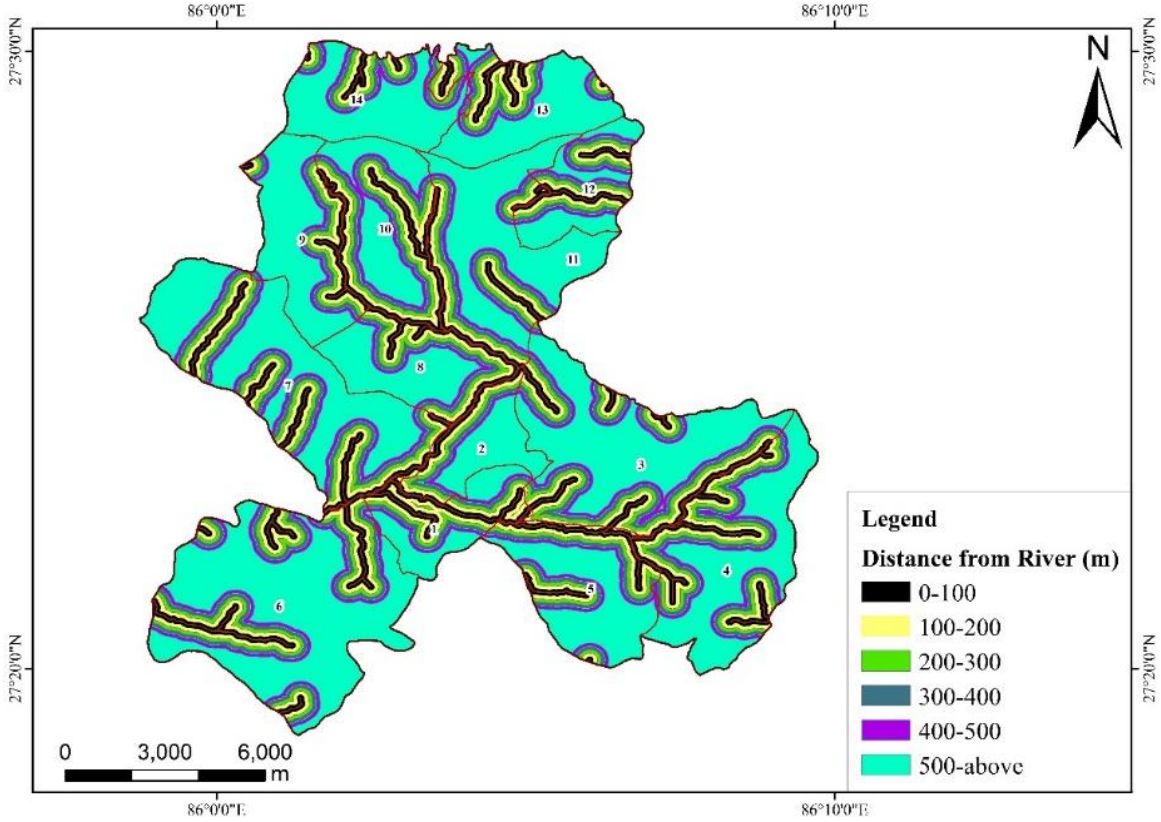

Figure 6. Distance from River map

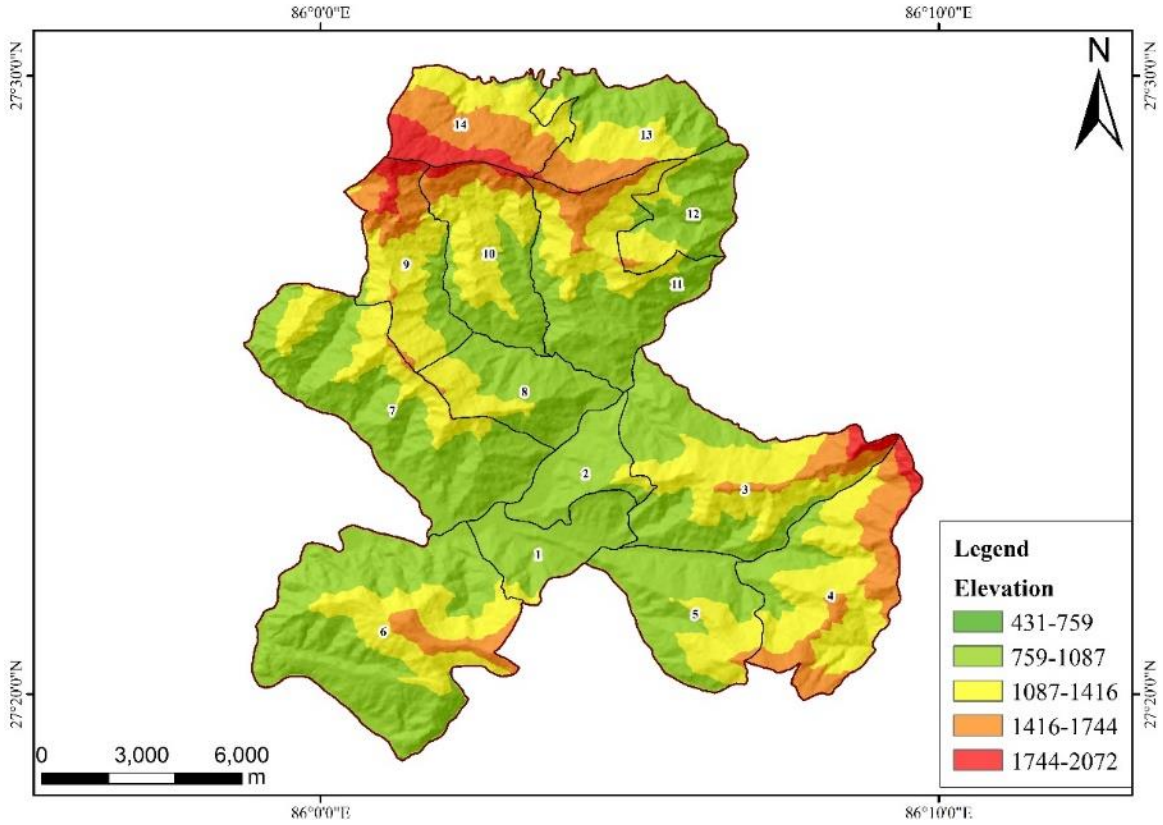

Figure 7. Elevation map

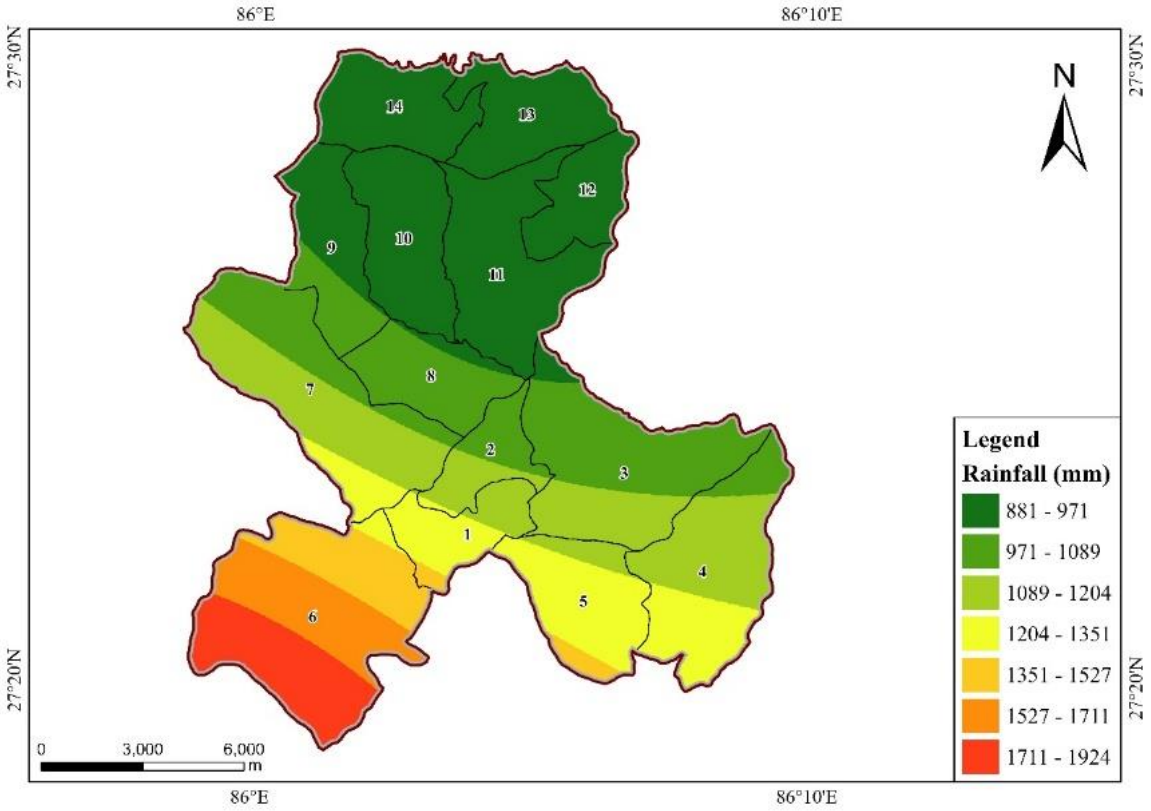

Figure 8. Rainfall map

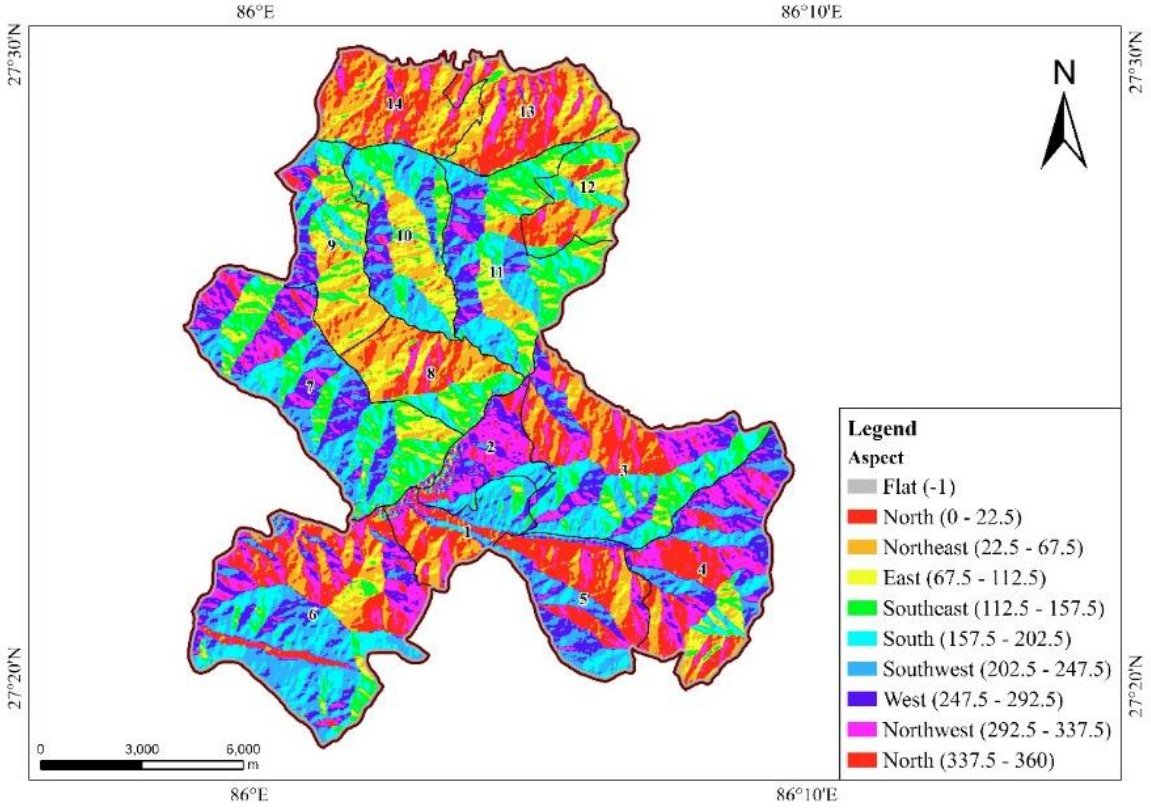

Figure 9. Aspect map

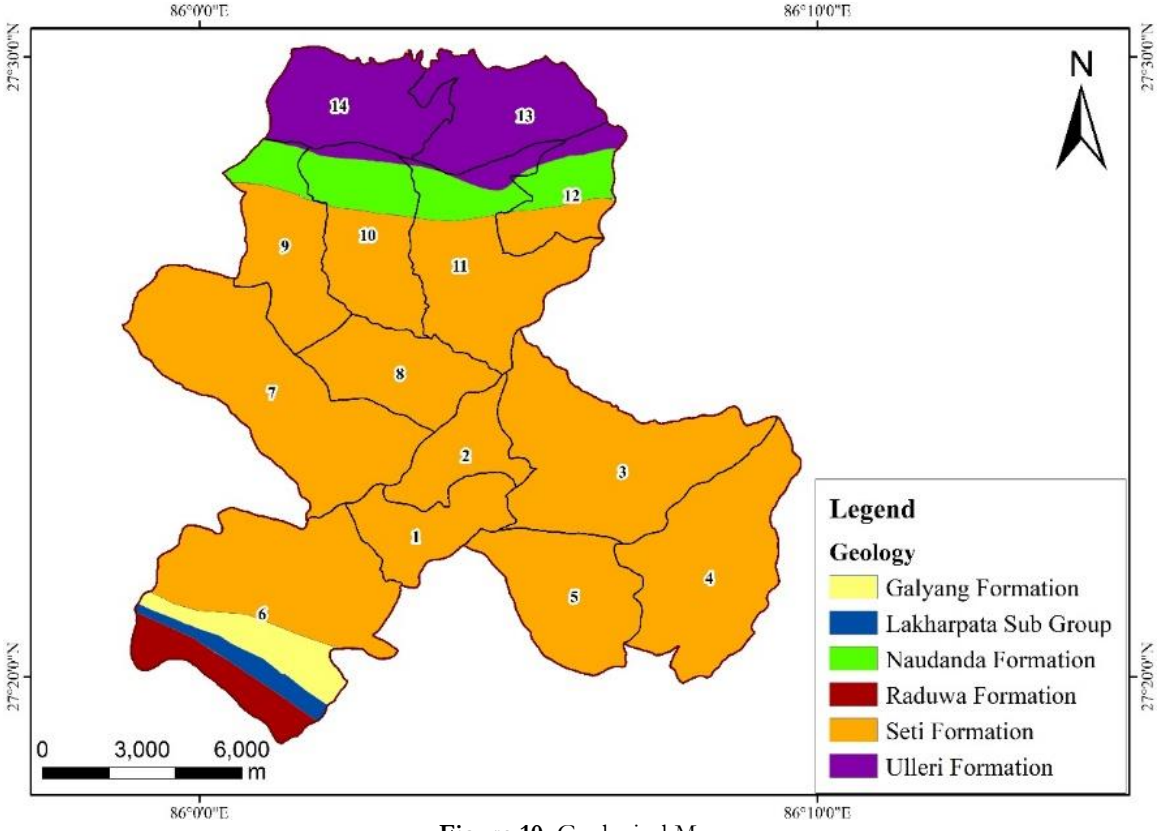

Figure 10. Geological Map

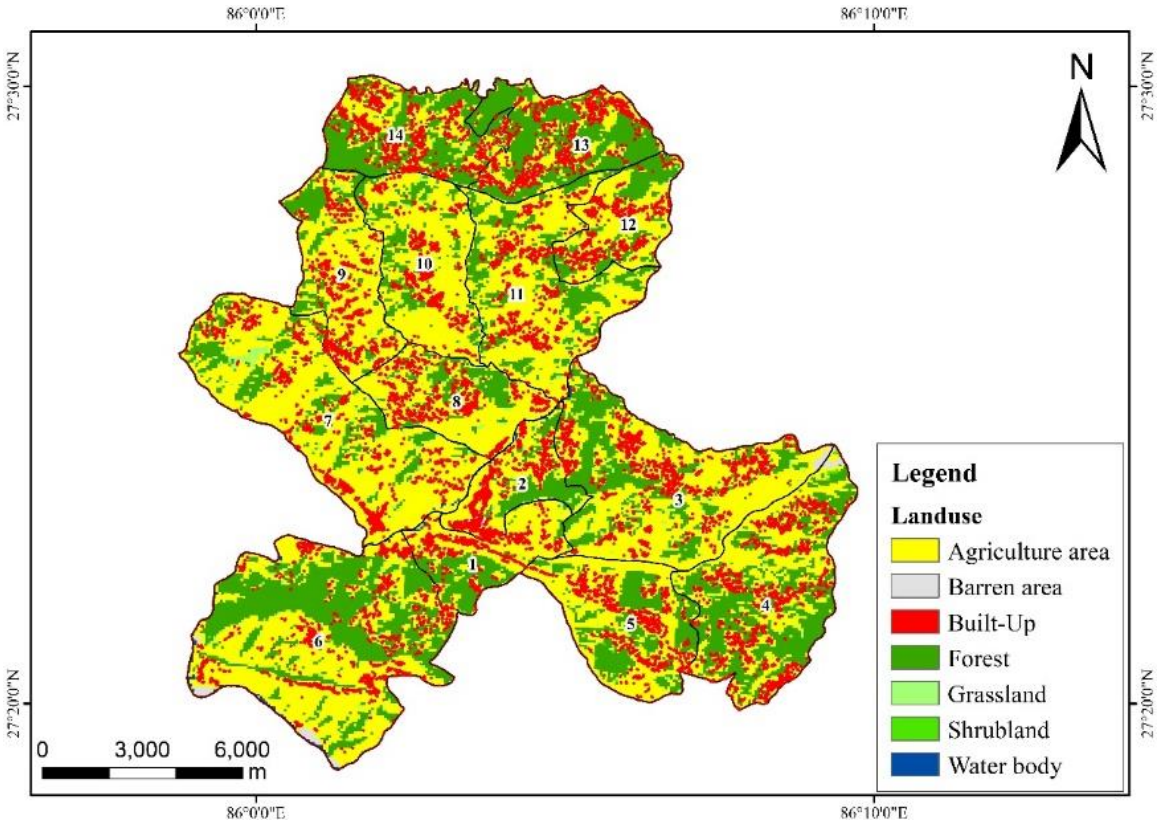

Figure 11. Land use map of the study area

Preparation of Landslide Susceptibility Map

Landslide susceptibility mapping necessitates the acknowledgment that the incidence and geographical distribution of landslides are influenced by multiple causal factors. Future landslides are anticipated to occur under conditions analogous to those of prior landslides (Lee & JA 2005). Assessing the probability of landslides necessitates a thorough comprehension of the particular physical conditions and initiating processes within the area of concern. This work utilized the Frequency Ratio (FR) method, augmented by GIS methodologies and spatial data, to statistically evaluate landslide susceptibility (Pradhan & Lee, 2010; Chen et al., 2016). The FR technique is extensively acknowledged and efficiently employed for landslide susceptibility mapping (Thapa & Bhandari, 2019; Chen et al., 2016; Bhandari et al., 2024; Dhakal & Tamang, 2025). This method relies on measuring the correlation between the landslide inventory and its causative components (Reis et al., 2012).

The landslide susceptibility was assessed using the Frequency Ratio (FR) Model, as suggested by Lee and Pradhan (2007) and Thapa & Bhandari (2019). According to Lee and Pradhan (2007), the process of calculating a FR for a certain group of elements that influence landslides may be described as Equation below.

$$FR = \left(\frac{a}{b}\right) \Big/ \left(\frac{c}{d}\right) \qquad \text{Eq. (2)}$$

Where,

a is the count of pixels containing a landslide for each factor, b is the total count of landslides in the study area, c is the count of pixels in the class area of the factor, d is the count of total pixels in the study area, and FR is the frequency ratio of a class for the factor.

The ratio values derived from the FR method were utilized to give weight values to the classes within each component map. This process resulted in the creation of weighted factor thematic maps. These maps were then overlaid and numerically combined using a raster calculator to generate the Landslide Susceptibility Index (LSI) map, as described by Lee and Pradhan (2007), employing Equation (3).

$$LS = \sum(Fr1 + FR2 + \cdots \ldots FRn) \qquad \text{Eq. (3)}$$

Fr represents the frequency ratio of each type or range of factors. The FR values obtained from the calculations for each pixel in the LSI provide an indication of the relative vulnerability to the occurrence of landslides. Higher pixel values of LSI indicate more susceptible to landslides, whereas lower pixel values indicate low susceptibility. To categorize landslide susceptibility indicators, many approaches may be utilized, including the equal interval, the natural break, and the standard deviation (Ayalew & Yamagishi 2005). In this work, the natural break approach was chosen for identifying the landslide susceptibility indices since it is the most often used method (Irigaray et al. 2007). The landslide susceptibility indices were categorized into four distinct classifications, namely Low, Moderate, High, and Very High.

Validation Using AUC Curve

A validation process was conducted to assess and analyze the efficacy and predictive capabilities of the developed models. Validation aims to assess the accuracy of models and their capacity to predict future landslides. The evaluation of accuracy involved a comparison between the existing landslide dataset and the outcomes of landslide susceptibility, taking into account rate curves and the corresponding areas under these curves (Chung & Fabri, 1999). The success rate curve was generated by plotting the cumulative percentage of training landslide occurrences against the cumulative percentage area of the susceptibility map. The prediction rate curve was created by graphing the cumulative percentage of test landslide locations in relation to the cumulative percentage area of the susceptibility map. To generate the success rate curve for each LSI map, pixel values were initially sorted in descending order and subsequently divided into 100 equal intervals, with each interval representing a 1% cumulative range. The categorized maps were overlaid with the landslide inventory map, and the success rate curve was generated from the resulting cross-tabulated values. A comparable method was employed to derive the prediction rate curve. The frequency ratio model's effectiveness was assessed through the area under the curve (AUC) method (Kayastha et al., 2013).

In order to determine how well landslide prediction models work, the ROC curve is often used (Hong et al., 2018). The x-axis of the ROC curve shows the false-positive rate (1-specificity), while the y-axis shows the sensitivity. Graphs representing the study's findings are generated by plotting the y-axis, which represents the cumulative proportion of landslide pixels, against the x-axis, which represents the cumulative proportion of the instability index. One way to compare the accuracy of different landslide models is by looking at their area under the curve (AUC). The area under the curve (AUC) is a measure of the model's predictive power; values closer to 1 indicate better performance (Hong et al., 2018; Lee et al., 2020).

There are several ways that may be employed to classify signs of landslide vulnerability, such as the equal interval, the natural break, and the standard deviation (Ayalew & Yamagishi, 2005). The natural break methodology was used as the method for determining landslide susceptibility indicators in this study due to its widespread usage (Irigaray et al., 2007). The susceptibility indices for landslides were classified into four separate categories: Low, Moderate, High, and Very High.

Results and Discussion

Landslide Inventory Map

Landslide susceptibility mapping is to develop an inventory map based on previous landslides. For

predicting future landslides, the accuracy of the data is strongly reliant on past and present landslides (Reichenbach et al. 2018). Figure 12 shows a landslide inventory map of the Manthali Municipality. Altogether 142 landslides, including small and very large, were noted in the area where 100 landslides were taken for train and 42 landslides for test data.

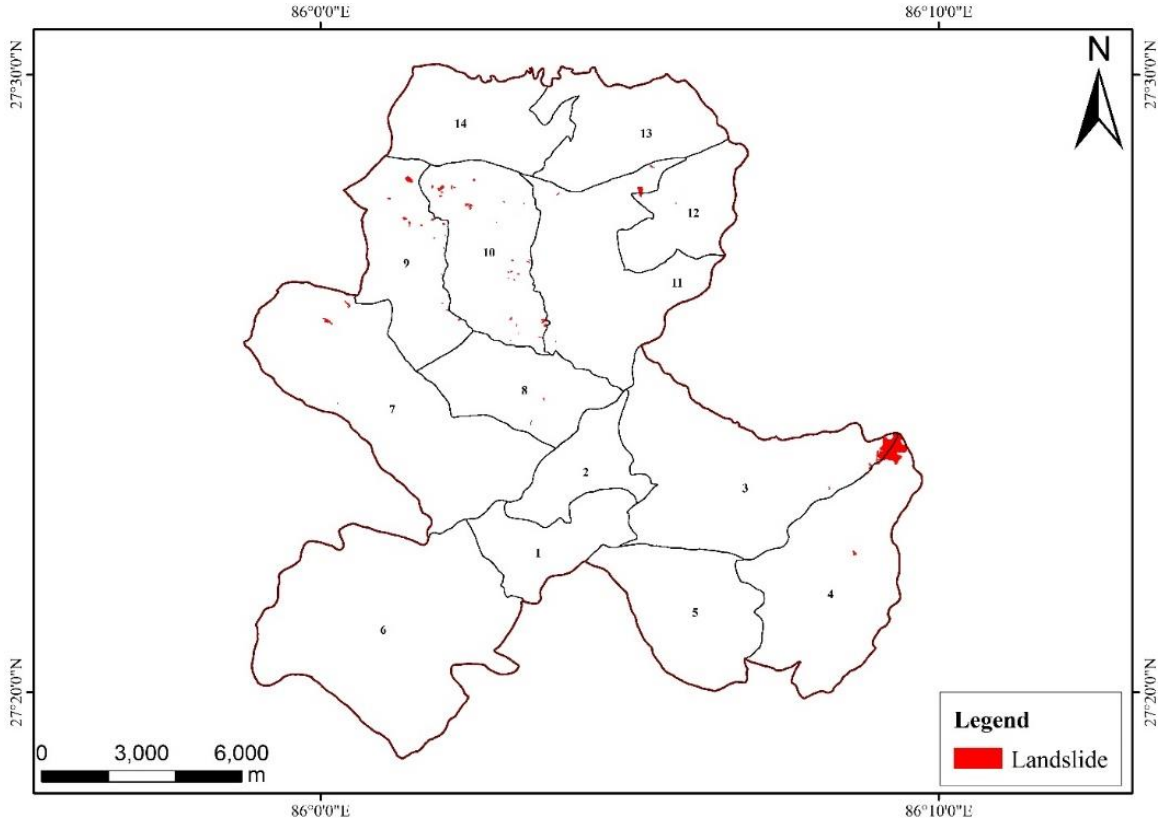

Figure 11. Illustration of Landslide in Manthali Municipality

Landslide and Triggering Factors

The factors contributing to landslides in this study exhibit values exceeding 1, indicating a positive correlation. A higher Frequency Ratio (FR) value indicates a more robust correlation between the factors contributing to landslides and their occurrence. FR values exceeding one indicate a strong correlation, whereas values below one suggests a weak correlation (Pradhan 2011). The findings indicate that the landslides within the study area were influenced by slope degrees exceeding 26.86 degrees in the southeast, south, southwest, and west aspects(Table 1). Thapa and Bhandari (2019) indicate that landslides exhibit a significant susceptibility correlated with slope degrees exceeding 30˚, particularly in the southeast, south, and southwest aspects. This finding aligns with the research conducted by Devkota et al. (2013), which identifies slope intervals of 35°–45° as being particularly vulnerable to landslides, followed closely by the 25°–35° slope class in the same directional aspects. In a comparable manner, the elevation range of 1415-2072 m, along with the surface structure characterized by both convex and concave forms, contributed to the occurrence of the landslide. The frequency ratios were determined to be 1.53 for concave surfaces and 1.14 for convex surfaces, respectively, demonstrating a significant correlation with the occurrence of landslides (Thapa & Bhandari 2019). Lee and Min (2001) assert that the structural characteristics of convex and concave surfaces play a significant role in the weathering process. In a comparable vein, a study by Bartelletti et al. (2017) reveals that, on average, 50 percent of landslides transpired in concave regions, while 30 percent were observed in convex regions. This indicates that concave slopes exhibit a heightened susceptibility to shallow landslides, attributed to the concentration of running water and the accumulation of pore pressure.

The proximity to the road reveals that the first class (0-101m) has a weight of 0.21, while the second class (101-200m) carries a weight of 0.42, both of which exhibit a positive correlation with the occurrence of landslides. As one moves away from the river, the initial class (0-101m) carries a weight of 0.50, thereby heightening the susceptibility to landslides. Landslides occur with regularity in regions that are distanced from roadways yet in close proximity to riverbanks. Concerning the geological factors, the Seti formation exhibits the highest FR value, significantly influencing landslide occurrence, closely followed by the Naudanda formation. Another element influencing the occurrence of landslides is precipitation. The precipitation exhibiting a FR value exceeding 1 exerted a more significant impact on landslide occurrences. The research undertaken by

Poudyal et al. (2010) has demonstrated an inverse correlation with landslide susceptibility, indicating that a greater prevalence of landslides occurs when the TWI is below 5. Our study corroborates this finding, revealing a similar inverse relationship with landslide susceptibility.

Subsequent to the amalgamation of these criteria, a landslide susceptibility classification was established, categorizing the locations into four distinct classes (Figure 13). A higher LSI value indicates increased susceptibility of the zone. The findings indicated that low, moderate, high, and very high classifications comprised 40.8%, 38.64%, 17.64%, and 2.92% of the overall research area, respectively.

Table 1. Frequency ratio distribution table

SN	*Type*	*Class*	*Class Pixels*	*% Class Pixels*	*Landslide Pixels*	*% Landslide Pixels*	*FR*
1	TWI	2.61-7.18	194214	83.12	550	85.27	1.03
		7.18-11.75	36004	15.41	90	13.95	0.91
		11.75-16.31	3005	1.29	5	0.78	0.60
		16.31-20.88	443	0.19	0	0.00	0.00
2	Slope	0-14	24713	10.58	9	1.40	0.13
		14-28	117740	50.39	86	13.33	0.26
		28-42	80596	34.49	255	39.53	1.15
		42-56	10396	4.45	263	40.78	9.17
		56-70	225	0.10	32	4.96	51.52
3	Curvature	Concave	37655	15.92	219	32.21	2.02
		Flat	140555	59.42	256	37.65	0.63
		Convex	58322	24.66	183	26.91	1.09
4	Distance from Road	0-100	132147	57.66	81	12.29	0.21
		101-200	52960	23.11	64	9.71	0.42
		201-300	24498	10.69	110	16.69	1.56
		301-400	12899	5.63	99	15.02	2.67
		401-500	6670	2.91	112	17.00	5.84
		>500	7186	3.14	193	29.29	9.34
5	Distance from River	0-100	57260	62.59	206	31.26	0.50
		100-200	51362	56.14	142	21.55	0.38
		200-300	43771	47.85	122	18.51	0.39
		300-400	34888	38.14	84	12.75	0.33
		400-500	25579	27.96	60	9.10	0.33
		>500	23500	25.69	45	6.83	0.27
6	Elevation	431-759	49180	20.81	12	1.82	0.09
		759-1087	78987	33.42	45	6.84	0.20

			1087-1416	74048	31.33	76	11.55	0.37
			1416-1744	27951	11.83	259	39.36	3.33
			1744-2072	6366	2.69	266	40.43	15.01
7		Rainfall	881-971	3902	1.66	0	0.00	0.00
			971-1089	4853	2.07	0	0.00	0.00
			1089-1204	7350	3.13	33	5.14	1.64
			1204-1351	43504	18.53	58	9.03	0.49
			1351-1527	112317	47.84	497	77.41	1.62
			1527-1711	38303	16.31	26	4.05	0.25
			1711-1924	24563	10.46	28	4.36	0.42
8		Aspect	Flat (-1)	740	0.32	0	0.00	0.00
			North	37932	16.23	1	0.16	0.01
			North East	30762	13.16	1	0.16	0.01
			East	21891	9.37	35	5.43	0.58
			South East	25883	11.08	155	24.03	2.17
			South	29312	12.54	171	26.51	2.11
			South West	30995	13.26	124	19.22	1.45
			West	26786	11.46	153	23.72	2.07
			North West	29369	12.57	5	0.78	0.06
9		Geology	Raduwa	5877	2.49	0	0.00	0.00
			Lakharpata	2912	1.23	0	0.00	0.00
			Galyang	14863	6.29	54	8.23	1.01
			Seti	5642	2.39	0	0.00	1.23
			Naudanda	176703	74.74	579	88.26	1.18
			Ulleri	30430	12.87	23	3.51	0.27
10		Land Use	Water	1800	0.31	33	1.26	4.07
			Forest	33300	5.75	989	37.88	6.59
			Grassland	0	0.00	3	0.11	0.00
			Agriculture	0	0.00	9	0.34	0.00
			Shrub land	155700	26.86	1289	49.37	1.84
			Built up	45900	7.92	260	9.96	1.26
			Bare	342900	59.16	28	1.07	0.02

The values for each element were generated, which were ultimately utilized to create the LSI map employing a raster calculator. The classification of the LSI into distinct categories that delineate susceptibility levels yields the Landslide Susceptibility Map. Table 1 presents an overview of the weight value computation utilizing the FR method.

Landslide Susceptibility Mapping

Creating a Landslide Susceptibility Model (LSM) represents a highly effective method for evaluating landslide risks and undertaking appropriate management duties. While various methodologies exist for the preparation of LSM, a definitive framework for model selection to achieve optimal LSMs remains absent (Nohani et al. 2019). The index of landslide susceptibility within the study area varied from 13 to 73, categorized into four principal classes of susceptibility (Fig.12). Areas with a notably high susceptibility are predominantly located within forests, aquatic environments, shrub land, and urbanized regions. The analysis reveals that the proportions of the low, moderate, high, and very high classes constitute 40.8%, 38.64%, 17.64%, and 2.92% of the overall study area, respectively. This study takes into account both intrinsic and extrinsic factors within this framework. The analysis revealed that factors such as slope, aspect, curvature, elevation, geology, land use, and rainfall significantly impacted the susceptibility to landslides in the region. Table 2 shows the frequency ratios for each factor class, obtained by dividing the landslide occurrences ratio by the area ratio.

The susceptibility map delineates the landslide-prone areas categorized into four classes: low, moderate, high, and very high. The extent of each category of landslide susceptibility map utilizing the FR approach is presented in Table 2 below. The extremely high susceptibility constituted merely 2.92% of the total. Approximately 79% of the region is occupied by low and moderate classes, indicating a minimal concern of landslides; nonetheless, numerous communities are situated within zones of high and very high susceptibility. Pathak and Devkota (2022) performed a study in the Rangun Khola watershed of far western Nepal, identifying susceptible zones that represent 19.74%, 18.29%, 18.68%, and 15.31% of the area, corresponding to moderate, low, very low, and very high susceptibility classes as defined by the FR method. Thapa and Bhandari (2019) reported that 17.3% and 3.68% of Barahakshetra Municipality in Sunsari District, Province No. 1, were classified as high and extremely high landslide susceptibility zones, respectively. Bhandari et al. (2024) evaluated four bivariate models for landslide susceptibility in the Siwalik hills of Nepal and observed no significant variations among the models, with the frequency ratio attaining over 70% success and prediction rate. Ayer and Bhandari (2024) performed a comparative analysis of the Weight of Evidence and Frequency Ratio models for landslide susceptibility in Purchaudi, Farwestern Nepal. They proposed that there is no substantial distinction between the two models, with the Frequency Ratio model exhibiting success and prediction rate surpassing 75%.

The validation involved comparing existing landslide locations with landslide susceptibility maps using both success rate and prediction rate curves. The success rate technique may assist in evaluating the efficacy of the landslide susceptibility maps in classifying regions with existing landslides (Bui et al. 2011; Pourghasemi et al. 2012). The prediction rate indicates the efficacy of the model and predictor variable in forecasting the landslide. This methodology is already widely employed to evaluate the efficacy of a predictive rule (Mohammady et al. 2012, Ozdemir & Altural 2013). The area beneath the curve for the frequency ratio model in our research demonstrated a success rate of 78.94% and a prediction rate of 74.06%. The success rate and prediction rate curves in this study are nearly indistinguishable, and the models employed demonstrated commendable accuracy in forecasting the landslide vulnerability of the area under investigation.

Validation of the result

The area beneath the Receiver Operating Characteristic (ROC) curve illustrates the models' accuracy concerning both their success rate and prediction rate. The success rate indicates the precision with which the generated landslide map recognizes current landslides, while the prediction rate assesses the map's capacity to anticipate possible future landslides (Huang et al. 2015). This research involved an assessment of the Frequency Ratio (FR) and Statistical Index (SI) models through the analysis of success rate and prediction rate curves. The correlation established between the landslide susceptibility map and the datasets (70%) facilitated the construction of the success rate curve, while the remaining test data (30%) were employed to develop the predictive rate curve. The ROC curves illustrated in Figure 13 depict the efficacy of the landslide susceptibility maps generated by the FR Model. The curves representing the success rate and prediction rate indicated values of 79.94% and 74.06%, respectively. The model's validation is evidenced by both its success and prediction rate, indicating its applicability within the study area.

Numerous research employed the success rate curve and predictive rate curve to corroborate the results obtained from the FR model. Regmi et al. (2014) utilized frequency ratio, weights of evidence, and statistical index models to compare landslide susceptibility mapping in the Central Nepal Himalaya. The FR model exhibited the highest performance, achieving a success rate of 76.8 percent and a predicted accuracy of 75.4 percent. The FR model attained a success accuracy of 75 percent and a forecast accuracy of 70 percent for landslide susceptibility assessment in a region of the Uttarakhand Himalaya, India (Pham et al. 2015). The study by Regmi et al. (2014) achieved success accuracy of 83.31% and prediction accuracy of 78.58% for landslide susceptibility mapping in the Bhalubang-Shivapur area of Mid-Western Nepal using the FR model. The area under the curve indicated success rates of 72.55% and 71.73% for percentage and prediction rate, respectively (Thapa & Bhandari 2019), demonstrating comparable results in both studies. The model employed in the research

exhibits commendable accuracy in forecasting the landslide susceptibility of the studied area. A comparable study by Acharya et al. (2017) in the Bhotang village development committee, Nepal, reported AUC values of 0.713 for validation, 0.725 for training, and 0.722 for the entire dataset in the FR model. Our findings are precise and largely consistent with the prior study, and the FR model is identified as an appropriate framework for landslide susceptibility mapping.

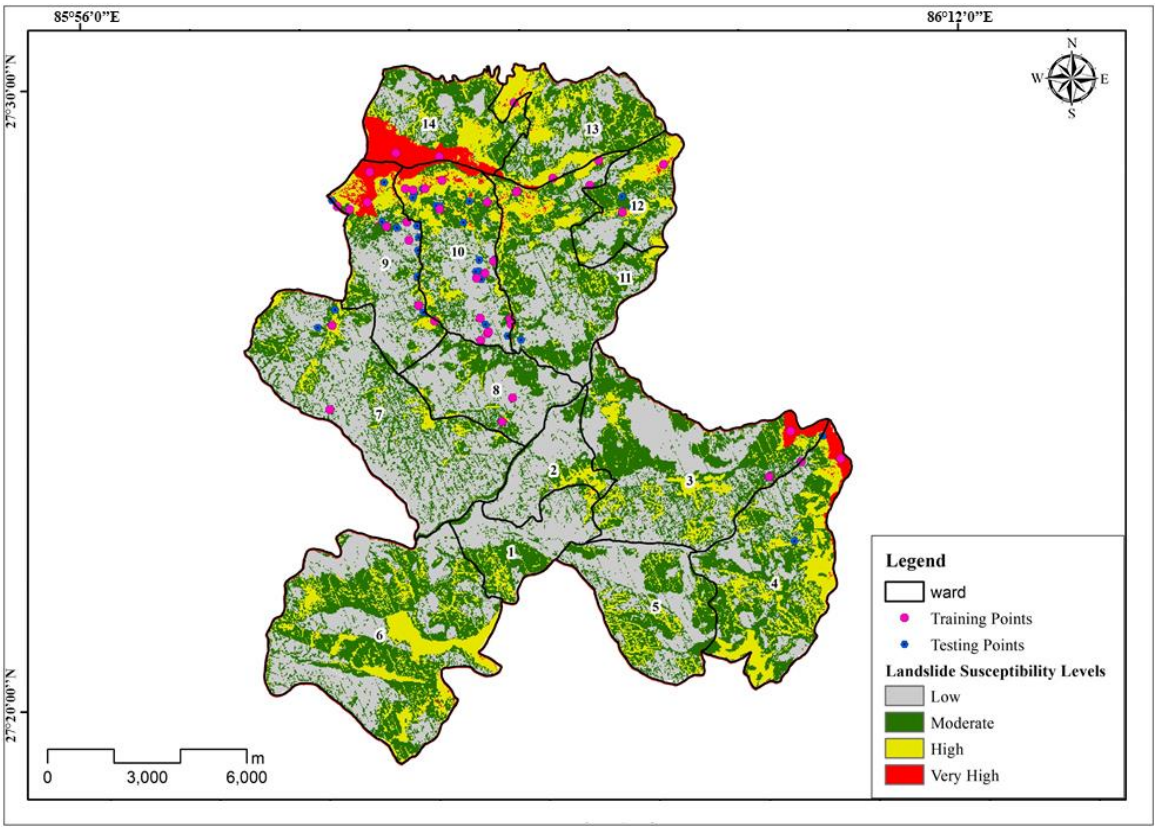

Figure 12. Landslide Susceptibility Map of the study area

Table 2. Illustration of Area Covered by each Landslide Susceptibility Classes

Class	Pixel Count	Area (in sq. m)	% Covered
Low	94956	8546.04	40.81
Moderate	89914	8092.26	38.64
High	41020	3691.8	17.63
Very High	6796	611.64	2.92
Total	**232686**	**20941.74**	**100**

Diverse methodologies exhibit differing levels of efficacy, either in their predictive capacity or in the implementation process. In certain instances, such as the Nepal Himalayas (namely Kathmandu, Mugling, and Gorkha), Logistic Regression (LR) has demonstrated prediction rates over 82% (Dahal, 2014). Gautam et al. (2021) achieved a superior prediction rate of 86.9% in the severely mountainous terrain of Sindhupalchowk district utilizing the Artificial Neural Network (ANN) approach. Ayer and Bhandari (2024) achieved comparable success and predictive accuracy from both the weight of evidence (WoE) and frequency ratio (FR) models. Regmi et al. (2014) achieved comparable results from the FR and WoE models. Kayastha et al. (2012) employed the analytical hierarchy process (AHP) in the Kaligandaki hydrocatchment and the Tinau watershed, achieving a success rate of up to 77.54%. Numerous researchers have employed AUC-ROC curves for model validation in the Nepal Himalaya to assess landslide susceptibility outcomes (Dahal et al., 2013; Regmi et al., 2014; Kayastha et al., 2012; Thapa and Bhandari, 2019; Pokharel & Bhandari, 2019; Bhandari et al., 2024; Ayer & Bhandari, 2025).

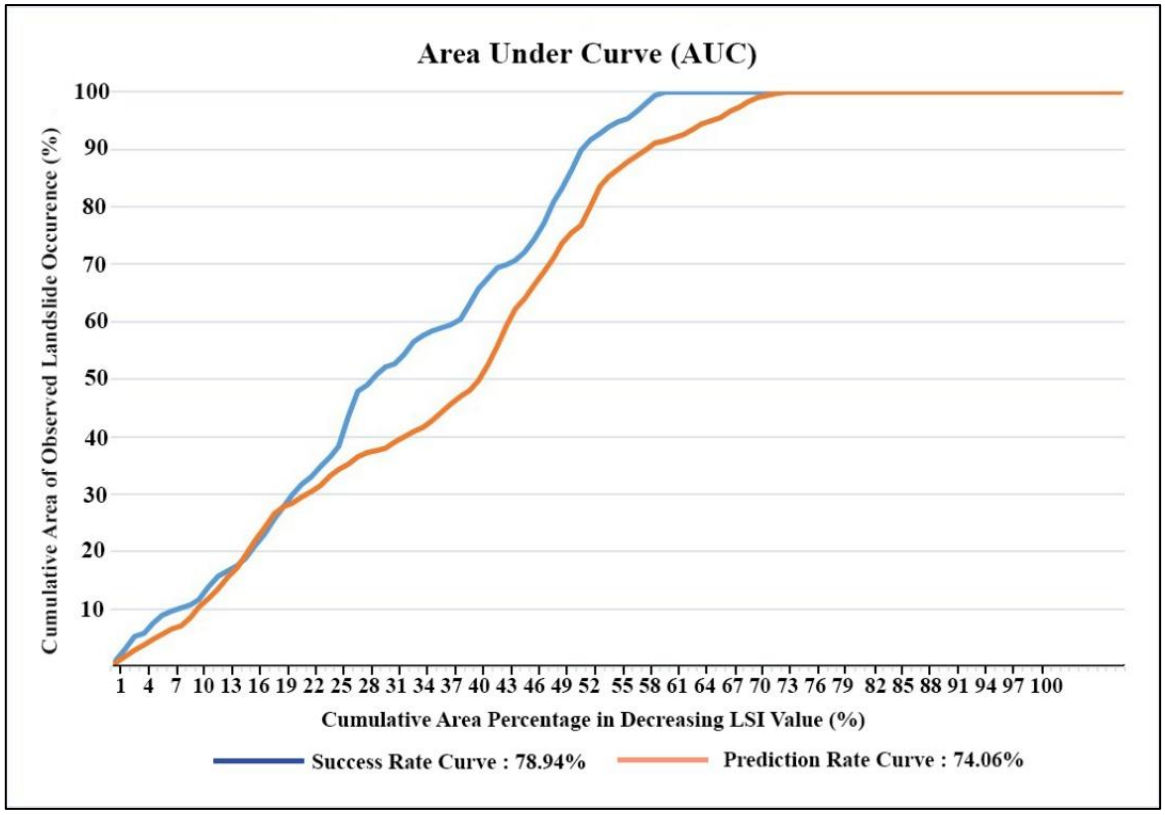

Figure 13. Area under curve (AUC) using the validation and training datasets

Conclusions

The study was conducted by combining a GIS-based technique with a statistical bivariate method. The Frequency Ratio (FR) bivariate statistical modelling methodology was employed in the evaluation of landslide susceptibility in Manthali Municipality, Bagmati Province, Nepal. Total of 64 landslides locations were found using Google Earth digitizing and field surveys, which were then utilized to build a landslide inventory map of the study region. Out of the total landslide polygons, 70% (45) were utilized for training, while the remaining 30% (26) were used for validation. The results showed that the FR model has a success rate of 78.94 % and a prediction rate of 74.06 %. The AUC value of this model is reasonably high with model predictions, the findings of landslide susceptibility modelling are accurate and may be utilized in real-world landslide risk and vulnerability assessments. The findings of this study can be utilized to forecast future landslides. It can also be useful in planning infrastructure development and relocation initiatives. As a result, such research may be extremely useful to land use planners, policymakers, and implementing agencies.

Acknowledgements: The authors express their gratitude to the local people, as well as the ward and municipal office of Manthali municipality, for their invaluable contributions of historical data regarding the landslide and its repercussions.

Author Contributions: BPB: Originated the proposed concept, meticulously examined the data, guided the process, and prepared the final manuscript; TAM: Meticulously gathered the data, developed the map and composed the initial draft of the manuscript.

Conflict of interest: The authors declare that they have no conflict of interest.

Data availability: The data of the current study is accessible upon reasonable request from the corresponding author.

References

Acharya, T.D., Yang, I.T., & Lee, D.H. (2017): GIS-based landslide susceptibility mapping of Bhotang, Nepal using frequency ratio and statistical index methods. *Journal of the Korean Society of Surveying, Geodesy, Photogrammetry and Cartography*, 35(5), 357-364.

Addis, A. (2023). GIS-Based landslide susceptibility mapping using frequency ratio and Shannon Entropy Models in Dejen District, Northwestern Ethiopia. *Journal of Engineering*, 2023(1), 1062388.

Ayalew, L., & Yamagishi, H. (2005). The application of GIS-based logistic regression for landslide susceptibility mapping in the Kakuda-Yahiko Mountains, Central Japan. *Geomorphology*, 65(1-2), 15-31.

Ayer, P.B., & Bhandari, B.P. (2024). Landslide Susceptibility Mapping Using Frequency Ratio and Weight of Evidence Models in Purchaudi Municipality, Baitadi District, Nepal. *Nepal Journal of Environmental Science*, 12(2), 59-72.

Bartelletti, C., Giannecchini, R., D'Amato Avanzi, G., Galanti, Y., & Mazzali, A. (2017). The influence of geological–morphological and land use settings on

shallow landslides in the Pogliaschina T. basin (northern Apennines, Italy). *Journal of Maps*, 13(2), 142-152.

Beven, K.J., & Kirkby, M.J. (1979). A physically based, variable contributing area model of basin hydrology/Un modèle à base physique de zone d'appel variable de l'hydrologie du bassin versant. *Hydrological sciences journal*, 24(1), 43-69.

Bhandari, B.P., & Dhakal, S. (2018). Lithological control on landslide in the Babai Khola watershed, Siwaliks zone of Nepal. *American Journal of Earth Sciences*, 5(3), 54-64.

Bhandari, B.P., & Dhakal, S. (2019). Topographical and geological factors on gully-type debris flow in Malai River catchment, Siwaliks, Nepal. *Journal of Nepal Geological Society*, 59, 89-94.

Bhandari, B.P., & Dhakal, S. (2020). Spatio-temporal dynamics of landslides in the sedimentary terrain: a case of Siwalik zone of Babai watershed, Nepal. *SN Applied Sciences*, 2, 1-17.

Bhandari, B.P., & Dhakal, S. (2021). A multidisciplinary approach of landslide characterization: A case of the Siwalik zone of Nepal Himalaya. *Journal of Asian Earth Sciences: X*, 5, 100061.

Bhandari, B.P., Dhakal, S., & Tsou, C.Y. (2024). Assessing the prediction accuracy of frequency ratio, weight of evidence, Shannon entropy, and information value methods for landslide susceptibility in the Siwalik Hills of Nepal. *Sustainability*, 16(5), 2092.

Bui, D.T., Lofman, O., Revhaug, I., & Dick, O. (2011). Landslide susceptibility analysis in the Hoa Binh province of Vietnam using statistical index and logistic regression. *Natural hazards*, 59, 1413-1444.

Burrough, P.A., & McDonnell, R.A. (1998) *Principles of Geographical Information Systems*, Oxford, Oxford University Press, 330 pp.

Burt, T.P., & Butcher, D.P. (1986). Development of topographic indices for use in semi-distributed hillslope runoff models. *Zeitschrift für Geomorphologie. Supplementband*, 58, 1-19.

Chen, W., Chai, H., Sun, X., Wang, Q., Ding, X., & Hong, H. (2016). A GIS-based comparative study of frequency ratio, statistical index and weights-of-evidence models in landslide susceptibility mapping. *Arabian Journal of Geosciences*, 9, 1-16.

Chung, C.-J.F., & Fabbri, A.G. (1999) Probabilistic prediction models for landslide hazard mapping. *Photogrammetric Engineering & Remote Sensing*, 65(12), 1389–1399

Corominas, J., van Westen, C., Frattini, P., Cascini, L., Malet, J.P., Fotopoulou, S., ... & Smith, J.T. (2014). Recommendations for the quantitative analysis of landslide risk. *Bulletin of Engineering Geology and the Environment*, 73, 209-263.

Cruden, D. (1991). A simple definition of a landslide. *Bulletin of Engineering Geology & the Environment*, 43, 27-29.

Dahal, R.K. (2014). Regional-scale landslide activity and landslide susceptibility zonation in the Nepal Himalaya. *Environmental Earth Sciences*, 71, 5145-5164.

Dahal, R.K., Hasegawa, S., Nonomura, A., Yamanaka, M., Dhakal, S., & Paudyal, P. (2008). Predictive modelling of rainfall-induced landslide hazard in the Lesser Himalaya of Nepal based on weights-of-evidence. *Geomorphology*, 102(3-4), 496-510.

Dam, N.D., Amiri, M., Al-Ansari, N., Prakash, I., Le, H.V., Nguyen, H.B.T., & Pham, B.T. (2022). Evaluation of Shannon entropy and weights of evidence models in landslide susceptibility mapping for the Pithoragarh district of Uttarakhand state, India. *Advances in Civil Engineering*, 2022(1), 6645007

Devkota, K.C., Regmi, A.D., Pourghasemi, H.R., Yoshida, K., Pradhan, B., Ryu, I.C., ... & Althuwaynee, O.F. (2013). Landslide susceptibility mapping using certainty factor, index of entropy and logistic regression models in GIS and their comparison at Mugling–Narayanghat road section in Nepal Himalaya. *Natural hazards*, 65, 135-165.

Dhakal, S., & Tamang, N.B. (2025). Landslide Susceptibility Assessment in the Marin Khola Watershed of the Sub Himalaya, Central Nepal. *Journal of Institute of Science and Technology*, 30(1), 89-99.

Fell, R., Corominas, J., Bonnard, C., Cascini, L., Leroi, E., Savage, W.Z., & JTC-1 Joint Technical Committee on Landslides and Engineered Slopes. (2008). Guidelines for landslide susceptibility, hazard and risk zoning for land use planning. *Engineering geology*, 102(3-4), 85-98.

García-Rodríguez, M.J., Malpica, J.A., Benito, B., & Díaz, M. (2008). Susceptibility assessment of earthquake-triggered landslides in El Salvador using logistic regression. *Geomorphology*, 95(3-4), 172-191.

García-Rodríguez, M.J., Malpica, J.A., Benito, B., & Díaz, M. (2008). Susceptibility assessment of earthquake-triggered landslides in El Salvador using logistic regression. *Geomorphology*, 95(3-4), 172-191.

Gautam, P., Kubota, T., Sapkota, L.M., & Shinohara, Y. (2021). Landslide susceptibility mapping with GIS in high mountain area of Nepal: a comparison of four methods. *Environmental Earth Sciences*, 80(9), 359.

Germer, S., Kaiser, K., Bens, O., & Hüttl, R.F. (2011). Water balance changes and responses of ecosystems and society in the Berlin-Brandenburg region–a review. *DIE ERDE–Journal of the Geographical Society of Berlin*, 142(1-2), 65-95.

Hong, H., Liu, J., Bui, D.T., Pradhan, B., Acharya, T.D., Pham, B.T., ... & Ahmad, B.B. (2018). Landslide susceptibility mapping using J48 Decision Tree with AdaBoost, Bagging and Rotation Forest ensembles in the Guangchang area (China). *Catena*, 163, 399-413.

Irigaray, C., Fernández, T., El Hamdouni, R., & Chacón, J. (2007). Evaluation and validation of landslide-susceptibility maps obtained by a GIS matrix method: examples from the Betic Cordillera (southern Spain). *Natural Hazards*, 41, 61-79.

Irigaray, C., Fernández, T., El Hamdouni, R., & Chacón, J. (2007). Evaluation and validation of landslide-susceptibility maps obtained by a GIS matrix method: examples from the Betic Cordillera (southern Spain). *Natural Hazards*, 41, 61-79.

Kayastha, P., Dhital, M.R., & De Smedt, F. (2013). Evaluation of the consistency of landslide susceptibility mapping: a case study from the Kankai watershed in east Nepal. *Landslides*, 10, 785-799.

Khan, H., Shafique, M., Khan, M.A., Bacha, M.A., Shah, S.U., & Calligaris, C. (2019). Landslide susceptibility assessment using Frequency Ratio, a case study of northern Pakistan. *The Egyptian Journal of Remote Sensing and Space Science*, 22(1), 11-24.

Lee, S., & Pradhan, B. (2007). Landslide hazard mapping at Selangor, Malaysia using frequency ratio and logistic regression models. Landslides, 4, 33–41. doi:10.1007/s10346-006-0047-y.

Lee, D.H., Kim, Y.T., & Lee, S.R. (2020). Shallow landslide susceptibility models based on artificial neural networks considering the factor selection method and various non-linear activation functions. *Remote Sensing*, 12(7), 1194.

Lee, S., & Min, K. (2001). Statistical analysis of landslide susceptibility at Yongin, Korea. *Environmental Geology*, 40, 1095-1113.

Lee, S., & Talib, J.A. (2005). Probabilistic landslide susceptibility and factor effect analysis. *Environmental Geology*, 47, 982-990.

Lee, S., Choi, J., & Min, K. (2004). Probabilistic landslide hazard mapping using GIS and remote sensing data at Boun, Korea. *International Journal of Remote Sensing*, 25(11), 2037-2052.

Li, B., Liu, K., Wang, M., He, Q., Jiang, Z., Zhu, W., & Qiao, N. (2022). Global dynamic rainfall-induced landslide susceptibility mapping using machine learning. *Remote Sensing*, 14(22), 5795

Mohammady, M., Pourghasemi, H.R., & Pradhan, B. (2012). Landslide susceptibility mapping at Golestan Province, Iran: a comparison between frequency ratio, Dempster–Shafer, and weights-of-evidence models. *Journal of Asian Earth Sciences*, 61, 221-236.

Moore, I.D., Grayson, R.B., & Ladson, A.R. (1991). Digital terrain modelling: a review of hydrological, geomorphological, and biological applications. *Hydrological Processes*, 5(1), 3-30.

Nohani, E., Moharrami, M., Sharafi, S., Khosravi, K., Pradhan, B., Pham, B.T., ... & Melesse, A. (2019). Landslide susceptibility mapping using different GIS-based bivariate models. *Water*, 11(7), 1402.

Ozdemir, A., & Altural, T. (2013). A comparative study of frequency ratio, weights of evidence and logistic regression methods for landslide susceptibility mapping: Sultan Mountains, SW Turkey. *Journal of Asian Earth Sciences*, 64, 180-197.

Pal, S.C., & Chowdhuri, I. (2019). GIS-based spatial prediction of landslide susceptibility using frequency ratio model of Lachung River basin, North Sikkim, India. *SN Applied Sciences*, 1, 1-25.

Pathak, L., & Devkota, K.C. (2022). Landslide susceptibility assessment in the Rangun Khola watershed of far western Nepal. *Journal of Nepal Geological Society*, 63(01), 33-44.

Pham, B.T., Tien Bui, D., Indra, P., & Dholakia, M. (2015). Landslide susceptibility assessment at a part of Uttarakhand Himalaya, India using GIS–based statistical approach of frequency ratio method. *International Journal of Engineering Research & Technology,* 4(11), 338-344.

Pokhrel, K., & Bhandari, B.P. (2019). Identification of potential landslide susceptible area in the Lesser Himalayan Terrain of Nepal. *Journal of Geoscience and Environment Protection*, 7(11), 24-38.

Pourghasemi, H.R., & Rahmati, O. (2018). Prediction of the landslide susceptibility: which algorithm, which precision? *Catena*, 162, 177-192.

Pourghasemi, H.R., Pradhan, B., & Gokceoglu, C. (2012). Application of fuzzy logic and analytical hierarchy process (AHP) to landslide susceptibility mapping at Haraz watershed, Iran. *Natural Hazards*, 63, 965-996.

Pradhan, B. (2011). Use of GIS-based fuzzy logic relations and its cross application to produce landslide susceptibility maps in three test areas in Malaysia. *Environmental Earth Sciences*, 63(2), 329-349.

Pradhan, B., & Lee, S. (2010). Landslide susceptibility assessment and factor effect analysis: backpropagation artificial neural networks and their comparison with frequency ratio and bivariate logistic regression modelling. *Environmental Modelling & Software*, 25(6), 747-759.

Reichenbach, P., Rossi, M., Malamud, B.D., Mihir, M., & Guzzetti, F. (2018). A review of statistically-based landslide susceptibility models. *Earth Science Reviews*, 180, 60-91.

Reis, S., Yalcin, A., Atasoy, M., Nisanci, R.E.C.E.P., Bayrak, T., Erduran, M.U.R.A.T., ... & Ekercin, S. (2012). Remote sensing and GIS-based landslide susceptibility mapping using frequency ratio and analytical hierarchy methods in Rize province (NE Turkey). *Environmental Earth Sciences*, 66, 2063-2073.

Seibert, J.A.N., Bishop, K.H., & Nyberg, L. (1997). A test of TOPMODEL'a ability to predict spatially distributed groundwater levels. *Hydrological Processes*, 11(9), 1131-1144.

Shafique, M., van der Meijde, M., & Khan, M.A. (2016). A review of the 2005 Kashmir earthquake-induced landslides; from a remote sensing prospective. *Journal of Asian Earth Sciences*, 118, 68-80.

Silalahi, F.E.S., Pamela, Arifianti, Y., & Hidayat, F. (2019). Landslide susceptibility assessment using frequency ratio model in Bogor, West Java, Indonesia. *Geoscience Letters*, 6(1), 10.

Thapa, D., & Bhandari, B. (2019) GIS-Based Frequency Ratio Method for Identification of Potential Landslide Susceptible Area in the Siwalik Zone of Chatara-Barahakshetra Section, Nepal. *Open Journal of Geology*, 9, 873-896. doi: 10.4236/ojg.2019.912096.

Yang, J. (2018). Landslide damage from extreme rainstorm geological accumulation layers within plain river basins. *Journal of Coastal Research*, 82, 1-11.

Zinko, U., Seibert, J., Dynesius, M., & Nilsson, C. (2005). Plant species numbers predicted by a topography-based groundwater flow index. *Ecosystems*, *8*, 430-441.